Touch Probe Tip Compensation Using a Novel Transformation Algorithm for Coordinate Measurements of Curved Surfaces

DOI: XXX-XXX-XXXX

Touch Probe Tip Compensation using a Novel Transformation Algorithm for Coordinate Measurements of Curved Surfaces

Hee Kyung Ahn[1,#], Hyukmo Kang[2], Young-Sik Ghim[1] and Ho-Soon Yang[1]

1 Space Optics Team, Advanced Instrumentation Institute, Korea Research Institute of Standards and Science, 267 Gajeong-ro, Yuseong-gu, Daejeon, South Korea, 34113
2 College of Optical Sciences, University of Arizona, 1630 E. University Blvd., Tucson, AZ, USA, 85721
Corresponding Author / E-mail: hk.ahn@kriss.re.kr, TEL: +82-42-868-5947

KEYWORDS : Coordinate Measuring Machine, CMM, Free-form optics, Probe tip radius compensation

A transformation algorithm compensating a radius of the probe tip and pre-travel errors is proposed to improve measurement uncertainty of a coordinate measuring machine (CMM). The transformation algorithm does not only compensate a radius of the probe tip, but it also compensates a slipping displacement from the predicted contact point caused by vertical tension for each data point. The performance of the transformation algorithm was successfully demonstrated by applying the transformation algorithm to raw data of an on-axis lens and an off-axis mirror measured with the CMM and comparing them with a reference data measured with UA3P-5 having several tens of nanometer accuracy.

Manuscript received: August XX, 201X / Accepted: August XX, 201X
Manuscript received: August XX, 201X / Accepted: August XX, 201X

NOMENCLATURE

(x, y, z) = coordinates of measured point
(x_c, y_c, z_c) = coordinates of the predicted contact point
(x_c', y_c', z_c') = coordinates of the predicted contact point
r = distance from the origin to the measured point in xy plane
r_b = probe tip radius
R = radius of curvature of the test surface
k = conic constant of the test surface
θ = slope of the test surface
ϕ = azimuthal angle in the xy-plane
(T_x, T_y, T_z) = translation in x-, y-, z-axes
(R_x, R_y, R_z) = rotation about x-, y-, z-axes
(dx, dy, dz) = differences between measured data and target data in x-, y-, z-axes

1. Introduction

A Coordinate Measuring Machine (CMM) is a measurement instrument widely used in various manufacturing processes including the fabrication of turbine blade, car model development and surface milling [1]. It has also been employed in the aerospace and automotive industries, especially for measuring curved surfaces such as aspheric or free-form surfaces [2,3].

CMM can be classified into two main categories, contacting CMM and non-contacting CMM. Of the two, contacting CMM is more highly favored than non-contacting CMM because it provides higher accuracy. Furthermore, non-contacting CMM has some disadvantages when it measures diffusing surfaces such as ground mirrors or surfaces with limited viewpoints due to optical occlusions [4].

Nevertheless, when using contacting CMM, to maintain its original accuracy, probe radius compensation needs to be performed [1-2,5-18]. This is because the CMM can only read the coordinates of the center of the probe tip called indicated measured points, not those of the actual contact point [2,16-17].

When a computer-aided design (CAD) model of the testing surface is provided, the normal vectors along the surface can be easily calculated so that the testing surface can be accurately measured by approaching the probe toward its normal vectors. In this case, users can determine the coordinates of the measurement point by simply considering the radius of the probe tip, since the contact point is a tangent of the surface. There are a lot of correction methods based on the CAD model [13-15].

However, when the testing surface is unknown so the CAD model is not given in advance, the user cannot obtain the normal vectors of the surface. To overcome this problem, other methods such as compensation using a force sensor [11-12] have been studied, but for these hardware-focused approaches, expensive sensors which have many degrees of freedom are needed. Alternatively, software-focused

compensation approaches have been developed such as using the information on the reciprocal position of the adjacent indicated measured points [6-10]. In this case, a normal vector for a specific indicated point can be calculated and radius compensations are performed to each indicated measured point. However, those compensations are incomplete since the direction of the modeled correction vector deviates from the corrected one [17]. Furthermore, the pre-travel errors [18] caused by slipping of the touch probe tip is not considered in those methods.

In this paper, we propose a novel transformation algorithm to accurately measure aspheric surfaces by compensating both the error from the radius of the probe tip and the pre-travel errors. Its performance was demonstrated by measuring an on-axis aspheric lens and an off-axis aspheric mirror using the algorithm and comparing the results with data measured by a UA3P-5 profilometer, which has nanometer accuracy. It is expected that the novel transformation algorithm can improve measurement accuracy by compensating probe tip radius and pre-travel error of the probe tip from slipping on a test surface when unknown test targets are measured.

2. Methods

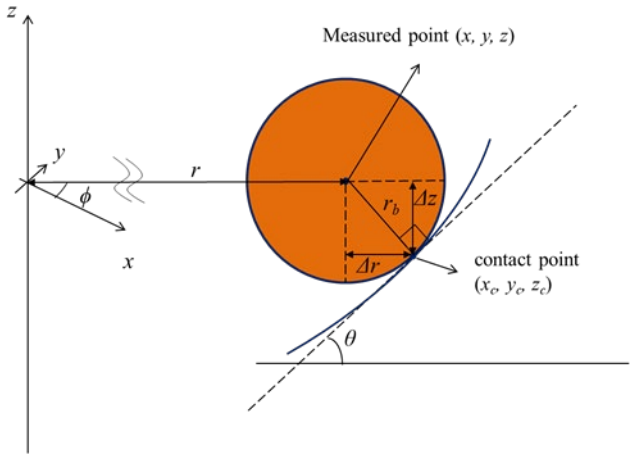

Fig. 1 Touch probe in the ideal case

As shown in Fig. 1, the coordinates of the contact point (x_c, y_c, z_c) which CMM users are interested in are different from the coordinates of the indicated measured point (x, y, z). They have a relationship as shown below [19]:

$$x = r\cos\phi, \quad y = r\sin\phi, \quad r = \sqrt{x^2 + y^2} \tag{1}$$

where ϕ represents the azimuthal angle in the x-y plane. The angle θ is assumed to be the derivative of the curve equation.

$$\tan\theta = df(r)/dr = r^2/(R - (k+1)f(r)) \tag{2}$$

where $f(r) = r^2/(R + \sqrt{R^2 - (k+1)r^2})$. $f(r)$ represents the aspheric equation of the testing surface, and R and k represent the radius of curvature and the conic constant of the surface, respectively. Therefore, the displacement Δr between the indicated measured point and the contact point in r direction, and the displacement Δz between the indicated measured point and the contact point in the z-direction are calculated below.

$$\Delta z = -r_b \cos\theta, \quad \Delta r = r_b \sin\theta \tag{3}$$

As a result, the coordinates of the contact point (x_c, y_c, z_c) are calculated below.

$$\begin{aligned} r' &= r + \Delta r, & x_c &= r'\cos\phi, \\ y_c &= r'\sin\phi, & z_c &= z + \Delta z \end{aligned} \tag{4}$$

However, the relationship is valid only in the ideal case. In practice, the contact point is not equal to the actual contact point since the probe stylus can be deformed and slipped while it is vertically moving down and contacting to the inclined surface. Consequently, the probe tip contacts the unwanted point (actual contact point), and there is a difference between the predicted contact point and the actual contact point (pre-travel errors). Fig. 2 shows the difference.

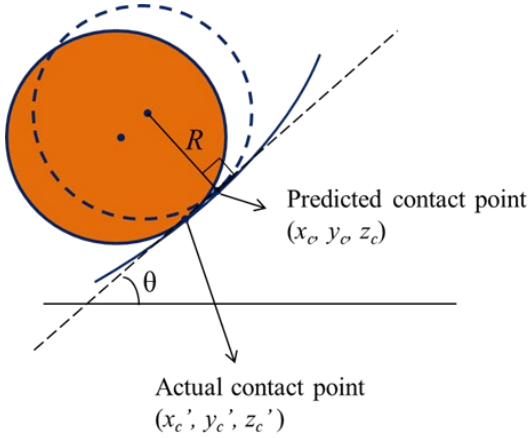

Fig. 2 The contact point error in practice

What concerns users are the predicted contact points, which are well-fitted with the target surface. Therefore, the coordinates of the actual contact point need to be compensated to the predicted contact point in order to fit the target surface well.

The pre-travel errors are treated as translations and rotations of the surface about the coordinate x, y, and z. The translations and the rotations of the surface can be expressed as a rigid-body motion including translation and rotation. In this case, the difference between the predicted contact point and the actual contact point can be counted as a displacement due to the rigid-body motion. The theoretical displacement $d\tilde{x}_i$, $d\tilde{y}_i$, $d\tilde{z}_i$ can be defined as below [20]:

$$\begin{aligned} d\tilde{x}_i &= T_x + z_i R_y - y_i R_z \\ d\tilde{y}_i &= T_y - z_i R_x + x_i R_z \\ d\tilde{z}_i &= T_z + y_i R_x - x_i R_y \end{aligned} \tag{5}$$

where x_i, y_i, z_i represent the coordinate of the i^{th} predicted contact point. T_x, T_y, T_z and R_x, R_y, R_z represent three translations and three rotations, respectively. Since we already know the coordinates of the actual contact point (the measured data) and the actual displacements dx, dy, dz (the differences between the measured data and the target data), we can obtain the coordinates of the predicted contact point by using a least-squares fit. Specifying ground mirrors as our target, the differences (i.e. the surface error of them) are about several μm to several tens of μm RMS. Therefore, the differences between the predicted contact points and the target data are negligible compared with the 3 mm diameter of the probe tip. The error E is defined as the difference between the actual displacement and the theoretical

DOI: XXX-XXX-XXXX

displacement which can occur by a linear combination of the translations and the rotations.

$$E = \sum_i w_i[(dx_i - d\tilde{x}_i)^2 + (dy_i - d\tilde{y}_i)^2 + (dz_i - d\tilde{z}_i)^2] \quad (6)$$

Here, dx_i, dy_i, dz_i represent the ith actual displacements. To obtain the minimum E, we took partial derivatives of E with respect to T_x, T_y, T_z, and R_x, R_y, R_z and set the result to zero.

$$\begin{aligned} &\partial E/\partial T_x = 0 \ \rightarrow \textstyle\sum_i w_i\left(T_x + z_i R_y - y_i R_z\right) = \sum_i w_i dx_i \\ &\partial E/\partial T_y = 0 \rightarrow \textstyle\sum_i w_i\left(T_y - z_i R_x + x_i R_z\right) = \sum_i w_i dy_i \\ &\partial E/\partial T_z = 0 \ \rightarrow \textstyle\sum_i w_i\left(T_z + y_i R_x - x_i R_y\right) = \sum_i w_i dz_i \end{aligned} \quad (7)$$

$$\begin{aligned} &\partial E/\partial R_x = 0 \rightarrow \textstyle\sum_i w_i(z_i dy_i - y_i dz_i) \\ &= \textstyle\sum_i w_i(z_i T_y + y_i T_z - (y_i{}^2 + z_i{}^2)R_x + x_i y_i R_y + x_i z_i R_z) \\ &\partial E/\partial R_y = 0 \rightarrow \textstyle\sum_i w_i(x_i dz_i - z_i dx_i) \\ &= \textstyle\sum_i w_i(-z_i T_x + x_i T_z + x_i y_i R_x - (z_i{}^2 + x_i{}^2)R_y + y_i z_i R_z) \\ &\partial E/\partial R_z = 0 \rightarrow \textstyle\sum_i w_i(y_i dx_i - x_i dy_i) \\ &= \textstyle\sum_i w_i(y_i T_x - x_i T_y + x_i z_i R_x + y_i z_i R_z - (z_i{}^2 + x_i{}^2)R_y) \end{aligned} \quad (8)$$

By summing the left terms and the right terms respectively, the above equations were developed further. For simplicity, we set the weighting factor w_i to be one.

$$\Sigma \begin{pmatrix} dx_i \\ dy_i \\ dz_i \\ z_i dy_i - y_i dz_i \\ x_i dz_i - z_i dx_i \\ y_i dz_i - x_i dy_i \end{pmatrix} =$$

$$\Sigma \begin{pmatrix} N & 0 & 0 & & 0 & z_i & -y_i & \\ 0 & N & 0 & & -z_i & 0 & x_i & \\ 0 & 0 & N & & y_i & -x_i & 0 & \\ 0 & z_i & y_i & -(y_i{}^2 + z_i{}^2) & x_i y_i & & x_i z_i & \\ -z_i & 0 & x_i & x_i y_i & & -(z_i{}^2 + x_i{}^2) & y_i z_i & \\ y_i & -x_i & 0 & x_i z_i & & y_i z_i & & -(x_i{}^2 + y_i{}^2) \end{pmatrix} \quad (9)$$

.

N represents the total number of points. As a result, we can obtain the three translations T_x, T_y, T_z, and three rotations R_x, R_y, R_z and compensate the coordinates of the actual contact points.

3. Experimental results

3.1 On-axis target

To prove the feasibility of the transformation algorithm for on-axis aspheric targets, we evaluated a target lens, which is an aspheric lens having a radius of curvature (ROC) R of 51.12 mm and a conic constant k of -0.575. The clear aperture (CA) of the lens is 90 mm and the material of the lens is N-BK7. Table 1 shows the information of the target lens in detail.

* Aspheric coefficients

	R	k	A_4	A_6	A_8	A_{10}
S1	51.12	-0.575	-4.837 e-11	-8.576 e-12	-2.014 e-15	-4.598 e-19
S2	Infinite	-	-	-	-	-

* Aspheric equation

$$Z = Y^2/R(1 + \sqrt{1 - (1+k)Y^2/R^2} + A_4 Y^4 + A_6 Y^6 + A_8 Y^8 + A_{10} Y^{10}$$

Table 1 The information of a target aspheric lens (on-axis).

Then, we measured the target lens by employing UA3P-5 (Panasonic) in Korea Basic Science Institute (KBSI), which has ±50 nm measurement accuracy [21]. Here, we did not measure the target lens by using interferometers since it needs specially designed optical components such as computer-generated hologram (CGH) to measure aspheric lenses. The ROC of the target surface was recorded to be 51.142 mm. We call this the reference data. An image of the target lens measured with the UA3P-5 is provided in Fig. 3.

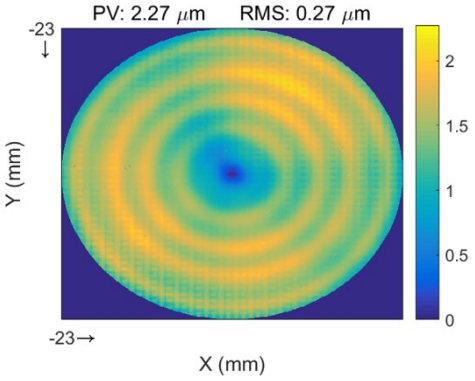

Fig. 3 An image of the target aspheric lens measured using UA3P-5

Afterward, we measured the target lens with a gantry type CMM (Dukin Co., Ltd.), which probe head is PH10M in Renishaw. The calibration results of the CMM provided by the manufacturer is shown in Table 2, which procedure was based on ISO10360-2.

Range (mm)	Measurement uncertainty (μm) (95% confidence level, k=2)
0	0.0
60	1.0
140	1.0
280	1.5
420	2.1
560	2.8

(a)

Range (mm)	Measurement uncertainty (μm) (95% confidence level, k=2)
0	0.0
60	0.9
140	1.3
280	1.7
420	2.4
560	3.1

(b)

Range (mm)	Measurement uncertainty (μm) (95% confidence level, k=2)
0	0.0
60	1.0
140	1.7

280	1.2
420	1.7
560	2.2

(c)

Table 2 Measurement uncertainties of the CMM: (a) in x-axis (b) in y -axis (c) in z-axis

After we measured the target lens with the CMM, we obtained the image of the target surface by applying the radius compensation (Fig. 4-(a)) and the transformation algorithm (Fig. 4-(b)). As a result, the recorded ROCs of the target surface applying those two algorithms were the same as 51.130 mm. However, the repeatability was somewhat different. The repeatability of the result applying the radius compensation was 3.6 μm while that of the result applying the transformation algorithms was 2.6 μm. The PV value difference in Fig. 4-(a), -(b) shows that the repeatability could affect the results. The difference between the reference ROC and the ROC of the results applying those two cases was about 13 μm.

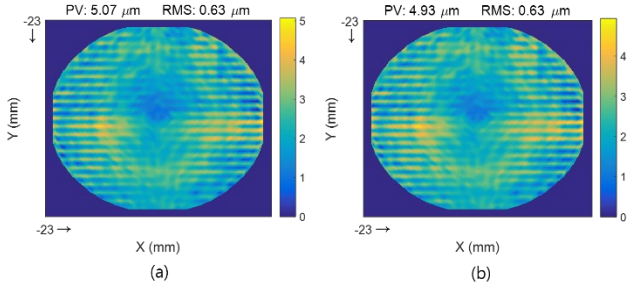

Fig. 4 Images of the target lens measured with CMM: (a) data applying the radius compensation only (b) data applying the transformation algorithm

3.2. Off-axis target

Fig. 5 The target surface (off-axis parabolic mirror, a = 48 mm)

In addition, we evaluated an off-axis target mirror to verify its performance for off-axis targets. The picture of the target parabolic mirror is shown in Fig. 5. The nominal ROC and the conic constant of the target mirror are 203.2 mm and -1, respectively. The CA of the target mirror is 90 mm and the material of the mirror is aluminum, which surface is coated with protected aluminum.

Then, we measured the target mirror by employing the UA3P-5 as well. The ROC of the target surface was recorded to be 203.2003 mm. An image of the target surface is depicted in Fig. 6.

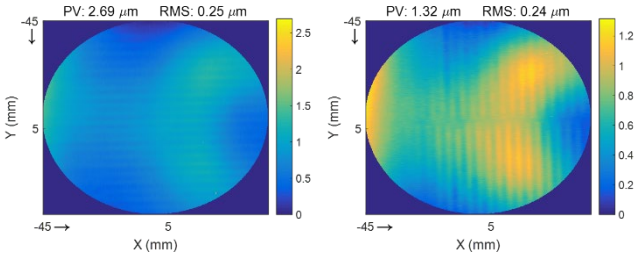

Fig. 6 Images of the target surface measured using UA3P-5: (a) raster scanned along x-axis, (b) raster scanned alogn y-axis

Afterward, we measured the target surface with the previously mentioned CMM and then obtained the two images by applying the two cases. The radius-compensated result and the result applying the transformation algorithm are shown in Fig. 7. In this case, the ROC of the radius-compensated result was 203.570 mm while the ROC of the result applying our algorithm was 203.194 mm. The gaps of the ROC between the reference and those two cases are about 370 μm and 6 μm, respectively. The result shows that the transformation algorithm is well-functioned in the case of the surface with slippery slopes. The repeatabilities of both cases were 3 μm and 1.9 μm, respectively.

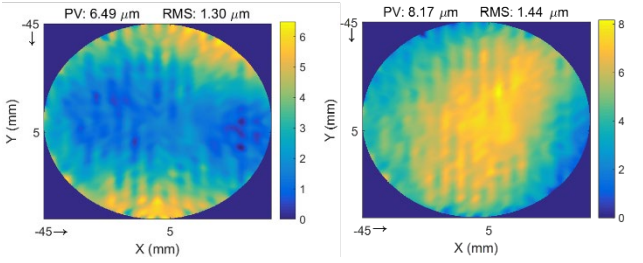

Fig. 7 Images of the target mirror measured with CMM: (a) data applying the radius compensation only (b) data applying the transformation algorithm

Considering the performance of the CMM, the additional error may have originated from the uncertainty of the conic constant and the error of the actual surface from target surface. Moreover, the fixed weighting factor (w_i = 1) could cause the error.

4. Conclusions

A transformation algorithm which can calculate predicted contact points by compensating the radius of the probe tip and deviation from pre-travel error was presented. The algorithm was applied to the raw data of an on-axis lens and an off-axis mirror measured with CMM. The results were compared with reference data from UA3P-5. In the case of an on-axis lens, the radius-compensated result and the result from the transformation algorithm have the same ROC, but the repeatability of the latter is somewhat better than that of the former.

The merit of the transformation algorithm was more obvious in the case of testing surfaces with steep slopes. In the case of an off-axis mirror, the differences between the reference ROC and the ROCs of the two cases were recorded to be 370 μm and 6 μm, respectively. Furthermore, the repeatability had the same tendency as in the case of the on-axis lens.

DOI: XXX-XXX-XXXX

From the above results, we concluded that by applying this transformation algorithm, when testing surfaces such as aspheric or free-form surfaces are unknown, they can be measured more accurately with the help the transformation algorithm by compensating the probe tip radius and by minimizing the error from slipping.

ACKNOWLEDGEMENT

This research was funded by Korea Research Institute of Standards and Science (KRISS-2018-GP2018-0014) and National Research Council of Science & Technology (NST) grant (MSIP) (No. CAP-12-04-KRISS) by the Korea government.

REFERENCES

1. Mayer, J. R. R., Mir Y. A., Trochu F., Vafaeesefat A. and Balazinski M., "Touch probe radius compensation for coordinate measurement using kriging interpolation," Proc. Instn. Mech. Engrs. Vol. 211, No. 1, pp. 11-18, 1997.
2. Ristic M., Ainsworth I. and Brujic D., "Contact probe radius compensation using computer aided design models," Proc. Instn. Mech. Engrs. Vol. 215, No. 6, pp. 819-834, 2001.
3. Li Y., Gu P., "Free-form surface inspection techniques state of the art review," Comput. Aided. Des. Vol. 36, No. 13, pp. 1395-1417, 2004.
4. Nicholls H. R., "Advanced Tactile Sensing for Robotics," 5th edition, World Scientific Publishing Co. Pte. Ltd., 1992.
5. Srinivasan S., Kovvur Y. and Anand S., "Probe Radius Compensation for On-Machine Measurement of Sculptured," ASME 2004 International Mechanical Engineering Congress and Exposition (IMECE) 2004-61838, pp. 913-920, 2004.
6. Liang R. and Lin A. C., "Probe radius compensation for 3D data points in reverse engineering," Comput. Indust. Vol. 48, No. 3, pp. 241–251, 2002.
7. Lin Y. C. and Sun W. I., "Probe radius compensated by the multi-cross product method in freeform surface measurement with touch trigger probe CMM," Int. J. Adv. Manuf. Technol. Vol. 21, No. 10-11, pp. 902–909, 2003.
8. Yin Z., Zhang Y. and Jiang S., "Methodology of NURBS surface fitting based on off-line software compensation for errors of a CMM," Precis. Eng. Vol. 27, No. 3, pp. 299–303, 2003.
9. Song C. K. and Kim S. W., "Reverse engineering: autonomous digitization of free-formed surface on a CNC coordinate measuring machine," Int. J. Mach. Tools Manuf. Vol. 37, No. 7, pp. 1041–1051, 1987.
10. Xiong Z. and Li Z., "Probe radius compensation of workpiece localization," J. Manuf. Sci. Eng. Vol. 125 100–104, pp. 2003.
11. Park J., Kwon K. and Cho N., "Development of a coordinate measuring machine (CMM) touch probe using a multi-axis force sensor," Meas. Sci. Technol. Vol. 17, No. 9 pp. 2380–2386, 2006.
12. Aoyama H., Kawai M. and Kishinami T., "A new method for detecting the contact point between a touch probe and a surface," Ann. CIRP, Vol. 38, No. 1, pp. 517–520, 1989.
13. Duffie N. A. and Feng S. C., "Modification of bicubic surface patches using least squares fitting techniques," Comput. Mech. Eng., Vol. 3, pp. 57–65 (CIME Research Supplement), 1985.
14. Ainsworth I., Ristic M. and Brujic D., "CAD-based measurement path planning for free-form shapes using contact probes," Int. J. Adv. Manuf. Technol., Vol. 16, No. 1, pp. 23–31, 2000.
15. Jeong J. and Kim K., "Generation of tool paths for machining free-form pockets with islands using distance maps," Int. J. Adv. Manuf. Technol., Vol. 15, No. 5, pp. 311–316, 1999.
16. Magdziak M., "An algorithm of form deviation calculation in coordinate measurements of free-form surfaces of products," Stroj. Vestn-J. Mech. E., Vol. 62, No. 1, pp. 51-59, 2016.
17. Wozniak A. and Mayer J. R. R., "A robust method for probe tip radius correction in coordinate metrology," Meas. Sci. Technol., Vol. 23, No. 2, pp. 025001, 2012.
18. Lee M. and Cho N.-G., "Probing-error compensation using 5 degree of freedom force/moment sensor for coordinate measuring machine," Meas. Sci. Technol., Vol. 24, No. 9, pp. 095001, 2013.
19. Zobrist T. L., "Application of laser tracker technology for measuring optical surfaces," dissertation, The University of Arizona, 2009.
20. Doyle K. B., Genberg V. L. and Michels G. J., "Integration of Optomechanical Analysis," SPIE Press, 2002.
21. https://www.panasonicfa.com/sites/default/files/pdfs/UA3P.pdf